Direct Simulation of Convective Adjustment and Other Ensemble Effects

David E. Dietrich
JAYCOR, *205 South Whiting Street, Alexandria, Virginia 22304*

[Manuscript received 29 April 1976, in revised form 5 October 1976]

ABSTRACT

Convective adjustment is studied using results from a two-dimensional numerical model (of a baroclinic, dry, rotating fluid) that, in contrast to parameterization approaches, uses the *full dynamic equations in spectral form* to determine interactions among large-scale quasi-geostrophic waves and small-scale eddy ensembles. Both the large-scale and the small-scale eddies result from *physical* instabilities. The spectral formulation has desirable energy propagation and conservation properties, and also has the advantage (not implemented in this early study) of allowing one to determine interactions between different scale eddies without having to represent intermediate scale eddies. The primary results are that: (i) there is a clear spectral gap in interactions affecting large-scale eddies and (ii) the large-scale vertical heat transport by the small-scale eddy ensembles varies significantly with time. This variation appears at least partly associated with ensemble group velocities in a *space*-varying large-scale environment, rather than with time variations of the large-scale environment (as would be consistent with the parameterization assumption that large-scale fields determine nonlinear transports by unresolved eddies).

1 Introduction

It is well established that ensembles of small-scale atmospheric eddies affect large-scale atmospheric eddies (scales of 1000 km or more) and vice-versa. The primary mechanisms for the former processes are vertical transports of heat and momentum and conversion between latent and sensible heat. The large-scale eddies, in turn, modulate the small-scale eddies. CISK is a widely discussed example of an important scale interaction (Charney and Eliassen, 1964; Ogura, 1964; Ooyama, 1964; Bates, 1973; Lindzen, 1974).

These phenomena have important nonlinear aspects and are not understood in detail. Recent power spectrum measurements (Högström and Högström, 1975) have shed new light on the mechanisms; the implied gap in the energy spectrum suggests that "nonlocal" spectral interactions discussed in this section are very active and may be predominant. The current AMTEX data (Ninomiya, 1975) are being gathered to gain more quantitative information on the primary

mechanisms. The main practical requirements are quantitative relations between large-scale vertical transports of heat and momentum and latent heat release (dependent variables), and large-scale fields (independent variables). Extensive and accurate measurements are required. I believe the present numerical approach can complement such data, and yield a detailed picture which is difficult to obtain purely from observational data.

Previous numerical studies have been primarily concerned with convection in a mesoscale environment and have focused on the detailed structure and physics of individual convection eddies and/or on the mesoscale space-averaged transport properties. The present study is more concerned with how an *ensemble* of small-scale convective eddies is modulated in space and time by nonlinear interaction with time-dependent large-scale eddies. The basic requirements for such a numerical study are that both long, quasi-hydrostatic, quasi-geostrophic waves (resulting from baroclinic instability), and short, non-hydrostatic, nonlinear waves (resulting from static and boundary-layer shear-induced instabilities) be modelled explicitly. The small-scale eddies must be determined by the Navier-Stokes equations, rather than by some greatly simplified physical relationships; the goal is to *improve* such parameterization relations. A spectral approach is very attractive, since it would: (i) allow one to represent widely separated scales of motion without having to represent intermediate scales, by using a "spectral gap" model; (ii) eliminate small-scale group velocity errors associated with linear phase speed errors. The latter are important because group velocity is a fundamental parameter in determining small-scale ensemble interactions with large-scale eddies (Dietrich, et al., 1975). Finite difference truncation error leads to large phase and group velocity errors in the small-scale flow components. It would (iii) allow conservation of energy in triad interactions between a long wave and two short waves, which is important in describing instability phenomena. Finite difference approaches do not allow such triad energy conservation because of the "aliasing" effects of truncation error. It would (iv) facilitate the quantitative description of the interactions among various scales of motion. It would (v) allow one to eliminate numerically troublesome high-frequency phenomena that do not influence large-scale eddies (Dietrich et al., 1975). Thus, a spectral approach is used in the present model, as described below.

A primary question is whether the most active interactions occur among widely separated scales of motion, with wave lengths differing by a factor of ten or more, or among relatively close scales of motion. The former interactions are spectrally "nonlocal" and characterize instability phenomena; the latter are "local" and characterize cascade phenomena. Since instability phenomena are such that the small-scale eddies have small time scales compared to the associated large-scale flow, it is reasonable to assume that the *effect* of the small-scale eddies on the large-scale eddies is in a kind of quasi-equilibrium dictated by the instantaneous state (and, perhaps, the very recent history) of the large-scale eddies. This is the basic assumption of parameterization methods, which specify the *effects* of unresolved small-scale eddies on the

resolved eddies in terms of the instantaneous state of the resolved eddies; the assumption is certainly valid for molecular transport phenomena, where the appropriate parameterization is simple diffusion; it is not yet clear just how well the assumption applies to large-scale effects of macroscopic mesoscale atmospheric eddies, but the assumption should be more nearly valid for instability phenomena than for cascade phenomena. This suggests that the large-scale components of flows with one or more "spectral gaps" (i.e. with widely separated bands in wave number space of actively interacting wave numbers, and relatively inactive gaps between the bands) are probably more predictable than those in "turbulent" flows dominated by cascade phenomena. Thus, the primary question of whether the dominant interactions are nonlocal is relevant to atmospheric predictability. Also, if they are nonlocal (other than the interactions among the energetic long waves), then application of a spectral gap approach might be possible in large-scale atmospheric forecast models. Finally, it should be noted that the significance of interactions affecting a large-scale wave depends on *whether they have a significant mean value on the time scale of the large-scale wave*; thus, the relative impact of "nonlocal" interactions which tend to remain in a given phase relative to the large-scale wave may be larger than instantaneous interactions may suggest.

2 The physical system

The physical system is a viscous, thermally conducting, Boussinesq, incompressible fluid between two rotating horizontal plates. The only y (latitudinal) dependence is an imposed linear temperature variation that is constant in space and time. (Temperature influences flow only through its *gradients*, so one can assume no further y-dependence.) Curvature terms are ignored. With appropriate choice of model parameters, eddies corresponding to baroclinic, static, and boundary-layer shear-induced instability occur. The baroclinic eddies are generally of much larger scale than the latter two types. The eddies equilibrate by: (i) vertical transports of heat and momentum; (ii) non-geostropic cascade of energy into dissipative, smaller horizontal-scale eddies; (iii) direct transfer of energy to much smaller-scale eddies. Although all eddies are affected by all three mechanisms, the baroclinically and statically unstable eddies of interest equilibrate mainly by vertical transports of heat, and the shear-induced eddies equilibrate mainly by vertical transports of momentum and by non-geostrophic energy cascade. In the atmosphere, there is, in addition to these mechanisms, quasi-geostrophic cascade of energy to smaller scales (Charney, 1971), and latitudinal transports of heat and momentum. The quasi-geostrophic cascade mechanism is associated with terms of the form $u'\partial(q')/\partial x$, where q is any variable whose tendency is relevant and the primes indicate eddy quantities (deviations from zonal averages). This mechanism is represented only by ageostrophic u' in the present model. The latitudinal transport mechanism associated with equilibration requires latitudinal variations not included in the present two-dimensional formulation. A quasi-geostrophic cascade mechanism could be included in a two-dimensional model by imposing an

x-variation of the latitudinal temperature gradient at the surface, such as that associated with land–sea differences, and by including an appropriate predictive equation for the latitudinal temperature gradient as well as for the temperature. However, the quasi-geostrophic cascade phenomenon in such a model would be associated with moderate large-scale divergence, while the atmosphere has important quasi-geostrophic cascade effects associated with the nondivergent component of horizontal flow. Thus, the importance of the quasi-geostrophic cascade mechanism in such a two-dimensional model may be different from its importance in the atmosphere. Williams (1967) uses a model similar to the present one, to study important non-geostrophic effects in high-Rossby-number late stages of frontal development. As he notes, nonlinear quasi-geostrophic effects are associated with the early low- and moderate-Rossby-number frontal development.

Using this simple model, some of the primary mechanisms of interest can be studied with greatly reduced cost and effort, while setting the groundwork for more efficient and more elaborate models (perhaps using a "spectral gap" approach). A specific relevant question is: just how complicated must the parameterization be in order to achieve acceptable representation of large-scale effects of small-scale eddies? If a very complicated scheme is necessary for accurate parameterization of the results of this model, then even more complicated schemes are probably required for the atmospheric interactions, and the use of a "spectral gap" model might prove more efficient in such a case.

The mathematical formulation of the laws governing the present simplified physical system is:

$$\left(\frac{d}{dt} + f\mathbf{k}\times\right)\mathbf{V} + \alpha_0\nabla\phi - g\beta\epsilon z\mathbf{j} - g\beta\,\hat{T}\mathbf{k} = \nu_{ex}\mathbf{V}_{xx} + \nu_{ez}\mathbf{V}_{zz}, \quad \text{(a)}$$

$$\frac{d\hat{T}}{dt} - \epsilon v = \kappa_{ex}\,\hat{T}_{xx} + \kappa_{ez}\,\hat{T}_{zz}, \quad \text{(b)} \qquad (1)$$

$$\nabla\cdot\mathbf{V} = 0, \quad \text{(c)}$$

where

$$\hat{T} = \hat{T}(x, z, t) = T(x, y, z, t) + \epsilon y$$

$$\frac{d}{dt} = \frac{\partial}{\partial t} + (\mathbf{V}\cdot\nabla)$$

$$\mathbf{V} = u\mathbf{i} + v\mathbf{j} + w\mathbf{k}$$

$$\nabla = \mathbf{i}\frac{\partial}{\partial x} + \mathbf{k}\frac{\partial}{\partial z}$$

$$p = \phi - (g\beta\epsilon/\alpha_0)yz$$

p is the usual non-hydrostatic pressure component, ϵ is the imposed constant latitudinal temperature gradient, β is a coefficient of thermal expansion, α_0 is the mean specific volume, which is assumed constant except in buoyancy terms,

and ν_{ex}, ν_{ez}, κ_{ex}, and κ_{ez} are horizontal and vertical-eddy transfer coefficients which are used to crudely parameterize even smaller-scale eddies than those explicitly resolved by the model. The model boundary conditions are:

$$\begin{aligned} \mathbf{V} &= 0 \text{ at } z = 0 \text{ and at } z = H, \\ \hat{T} &= 0 \text{ at } z = 0, \hat{T} = \sigma H \text{ at } z = H \end{aligned} \tag{2}$$

The flow is assumed periodic in x with a specified fundamental wave length.

3 The numerical formulation and procedure

For the reasons noted in the Introduction, the horizontal (x) variations of the fields are represented by Fourier series. In order to improve computational efficiency when high horizontal resolution is used, multiplications are performed in real space (using a fast Fourier transform algorithm to map between real and Fourier amplitude space). To assure that the products are non-aliased (and, thus, energy conserving), the number of real points used is *twice* the number of real Fourier amplitudes.[1] To facilitate accurate boundary-layer description while restricting the vertical resolution to *about* ten levels, a stretched vertical coordinate (z') is introduced:

$$z' = A \tan\left\{B\left(z - \frac{H}{2}\right)\right\} \tag{3}$$

where A is a normalizing coefficient and B is chosen such that roughly ¼ of the total change of z' occurs in the Ekman layer associated with the vertical eddy transfer coefficient ν_{ez}. A staggered grid (Williams, 1969), uniform in z', is used. Vertical derivatives are calculated using

$$\left.\frac{\partial(\,)}{\partial z}\right|_{z'=z'_i} = B\left(A + \frac{(z'_i)^2}{A}\right)\left.\frac{\partial(\,)}{\partial z'}\right|_{z'=z'_i} \doteq B\left(A + \frac{(z'_i)^2}{A}\right)\frac{(\,)_{i+\frac{1}{2}} - (\,)_{i-\frac{1}{2}}}{\Delta z'}. \tag{4}$$

Higher order derivatives are approximated using successive applications of the first *difference* approximation, thus conserving flux quantities. *All* linear terms are treated implicitly in time, using a trapezoidal (Crank-Nicolson) scheme. The nonlinear terms are treated using a forward time difference followed by a trapezoidal corrector. This allows a time step[2] six times greater than the Adams-Bashforth treatment of the nonlinear terms, with no significant increase in computation or storage. If all terms were treated implicitly using the trapezoidal rule, this would correspond to the numerical formulation given by Dietrich (1975) which conserves energy exactly in both space and time. The coupled linear implicit difference equations in z' are solved using a one-dimensional special case of the scheme described by Dietrich (1975).

[1]Non-aliased results can be obtained using a number of real points one and one-half times the number of Fourier amplitudes, thereby saving time over the algorithm used.

[2]The model time step used for the results discussed below is about one-half the vertical advection CFL during the most vigorous convection. This vigorous convection follows a period during which the vertical heat transport by the convective ensemble increases about 30 per cent per model time step.

The time marching is divided into three parts: (i) the wave-absent equations with initial conditions independent of x are integrated to a quasi-steady state; (ii) a few long waves are introduced through arbitrary temperature perturbations and low resolution equations are integrated until the waves are quasi-equilibrated; (iii) the high resolution equations are then integrated in time until quasi-equilibration is again achieved. The nonlinear terms drop identically from the equations for stage (i), since $w = 0$ and $\partial/\partial x = 0$.

Considerable savings are achieved by separating stage (iii), since a shorter time step *and* more computation per time step is required than in (i) or (ii). However, by using a more implicit vertical advection scheme (such as advocated by Dietrich et al., 1975), by subtracting out numerically troublesome high-frequency horizontally propagating modes (as described by Dietrich et al., 1975), and by utilizing a "spectral gap" approach advocated as here, it may be possible to greatly increase the computation efficiency in (iii), without significantly affecting the long-wave behaviour.

4 Results

Of primary interest in this study are high-resolution numerical experiments in which both large-scale quasi-geostrophic waves and small-scale convective boundary-layer eddies are resolved. However, several results from low resolution experiments are of interest as well.

a *Low Horizontal Resolution Cases* (With four or fewer waves)

In the second stage of the three-step time integration procedure described in Section 3, the longest represented wave (the fundamental Fourier mode) dominates the flow after sufficiently long time integration. Smaller-scale eddies are significant only when horizontal wavelengths comparable to the depth of the unstable boundary layer created by the large-scale flow are resolved in the third stage. Although the harmonics may temporarily dominate the flow because of their larger growth rates at the beginning of stage (ii), the fundamental continues to grow after the interior static stability increase caused by vertical eddy heat transport neutralizes the harmonics.[3] Eventually, the harmonics decay and the fundamental equilibrates, with some energy cascade into the harmonics. Such energy cascade maintains the harmonics at a much lower energy level than they originally attained as unstable modes in the mean flow, since it relies on inefficient non-geostrophic cascade of energy. (The energy cascade is associated with nonlinear products of the relatively small non-geostrophic part of the flow.) It should be noted that a sufficiently large increase of interior static stability implies destabilization of the boundary layers, since the upper and lower boundary temperatures are fixed in the present model. However, in the high-resolution results described below, the boundary-layer destabilization is due primarily to horizontal advection, not vertical heat transport.

A strong tendency for *steady* finite amplitude equilibration is found in low-resolution cases with Prandtl number, $Pr \equiv \nu_{ez}/\kappa_{ez}$, equal to one. For example,

[3]There is no beta-effect to stabilize long waves in the present model.

a case was run with $Pr = 1$, $Ro_T \equiv 2\pi(g\beta\epsilon H/f^2L) = 0.79$, and $Ek \equiv \nu_{ez}/fH^2 = 0.0005$, where Ro_T and Ek are thermal Rossby and Ekman numbers, and L is the fundamental wave length. *With two waves resolved* and 14 levels in a stretched vertical coordinate, the flow has a steady finite-amplitude equilibration. A similar case was run with ν_{ez} increased by a factor of ten, and all other parameters unchanged, so that $Ro_T = 0.79$, $Pr = 10$, and $Ek = 0.005$. In this case, the equilibration is very time dependent, with strong amplitude vacillation. These results appear superficially to be related to the diffusive destabilization phenomenon discussed by McIntyre (1968); however, his background flow does not have finite amplitude baroclinic waves which are present here.

b *Detailed Results from a Case with High Resolution*

A high resolution case was run with $Ro_T = 0.094$, $Pr = 10$, and $Ek = 0.0125$. Stage two of the integration resolved *four waves*. Stage three included *32 waves*, so the small-scale Rossby number is about 3. The small-scale horizontal wavelength is about twice the Ekman layer depth based on Ek. The vertical resolution was eleven levels in a continuously stretched vertical coordinate that magnifies boundary layer regions. The finite amplitude flow at the end of stage two is shown in Fig. 1(a). At the beginning of stage three, the newly resolved small-scale eddies are in a statically unstable large-scale environment, and the small-scale ensemble grows exponentially. The flow near the time of maximum small-scale activity is shown in Fig. 1(b). Fig. 2 shows the extremely rapid growth of the small-scale eddies (the e-folding time of the heat transport by the convective ensemble is about one model hour) during the early growth period. Figs 1(c) and 1(d) show the flow at times later in the stage three integrations.

Fig. 2 reveals a consistent relation between the large-scale vertical heat transport by the small-scale convective ensemble and large-scale flow parameters. Both the mean and wave number one components of the heat transport (curves E and F of Fig. 2) tend to grow when the boundary layer is relatively unstable (which is reflected by curves A and B being close together and C and D far apart[4]). This clear relation *suggests* that accurate parameterization may be possible in the present model with relatively simple parameterization relations. This may not be true for cases in which the convective heat transport has a more significant effect on the large-scale flow than in the present case. It is expected that, in the atmosphere, convective latent heat transport and release has a considerably more important effect than the sensible heat transport has in these results from the present dry model.

Curves E and F in Fig. 2 show the ensemble heat transport varying by about a factor of two even after the large initial adjustment. The dominant time scale is about one model day. The time dependence of the mean heat transport by a given wave number is even stronger, as suggested by the behaviour of wave numbers 23 and 24, shown in Fig. 3.

[4]The fact that curves *C* and *D* being far apart reflects an unstable boundary layer is related to the facts that the phase of the wave number one temperature field is nearly independent of height, and the amplitude increases toward mid-depth (see Fig. 1).

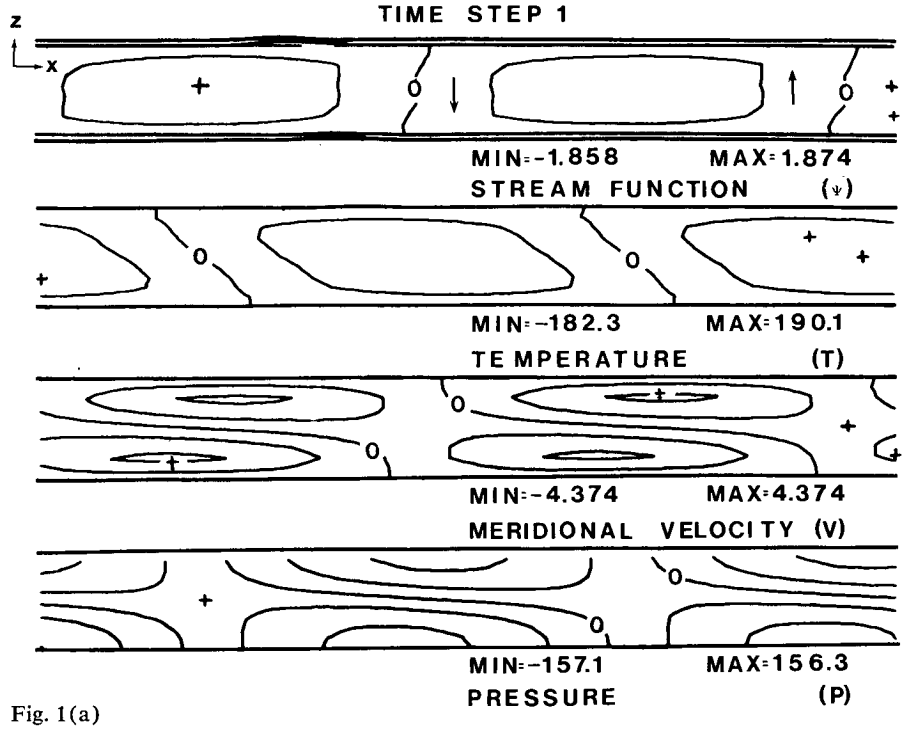

Fig. 1(a)

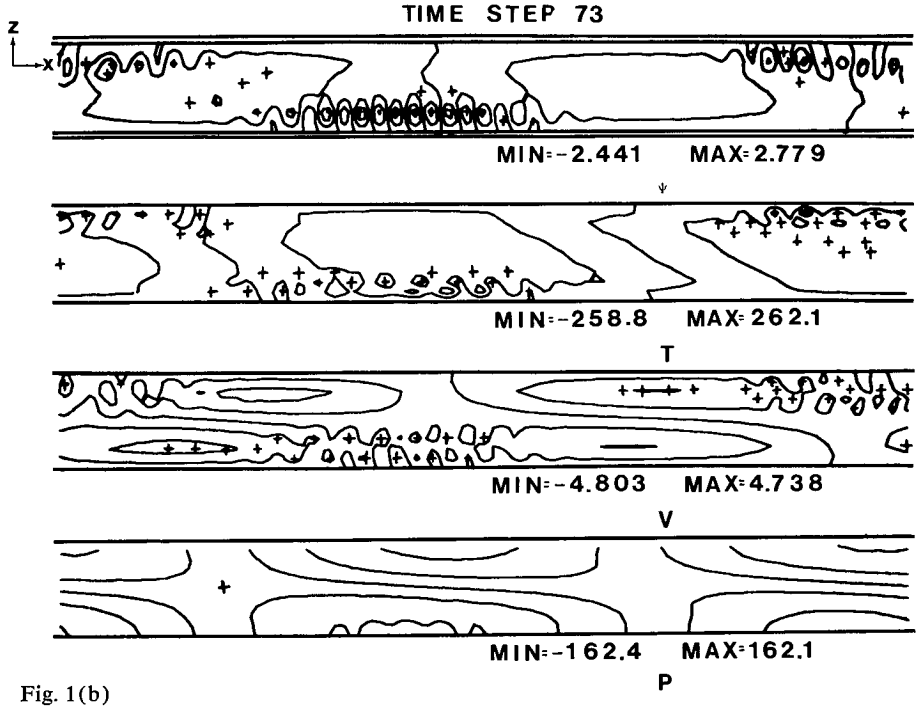

Fig. 1(b)

Fig. 1 Contour diagrams in $x - z$ planes showing eddy flow at time steps 1, 73, 97, and 177 of the stage-three (with 32 waves resolved) time integration. The time step is 1/96 day. Zonal (x) averages have been subtracted out to show eddy structure more clearly. The fields shown are: stream function for zonal overturnings (ψ);

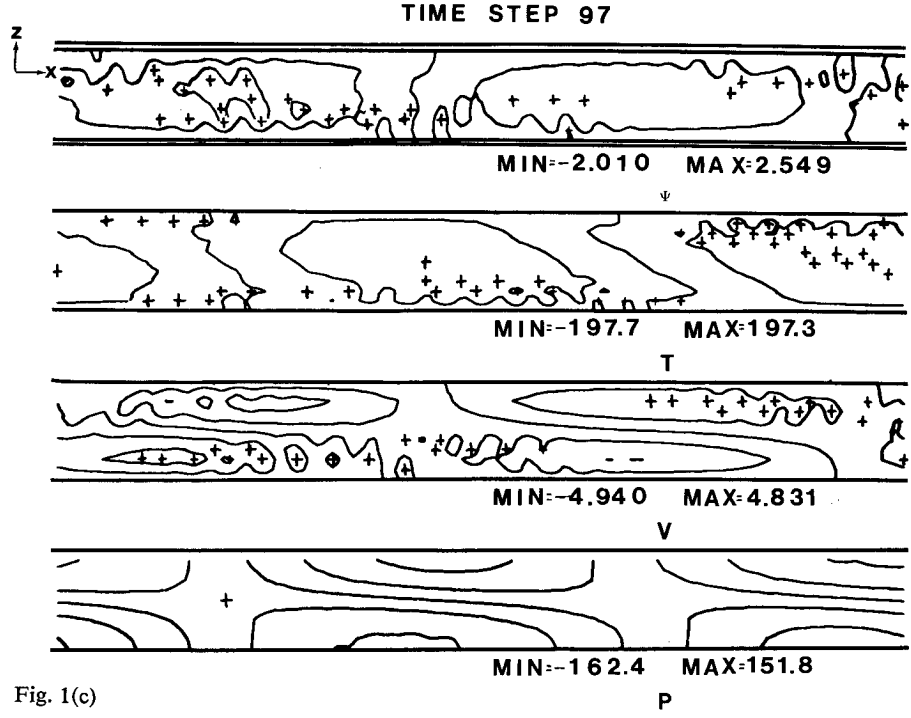

Fig. 1(c)

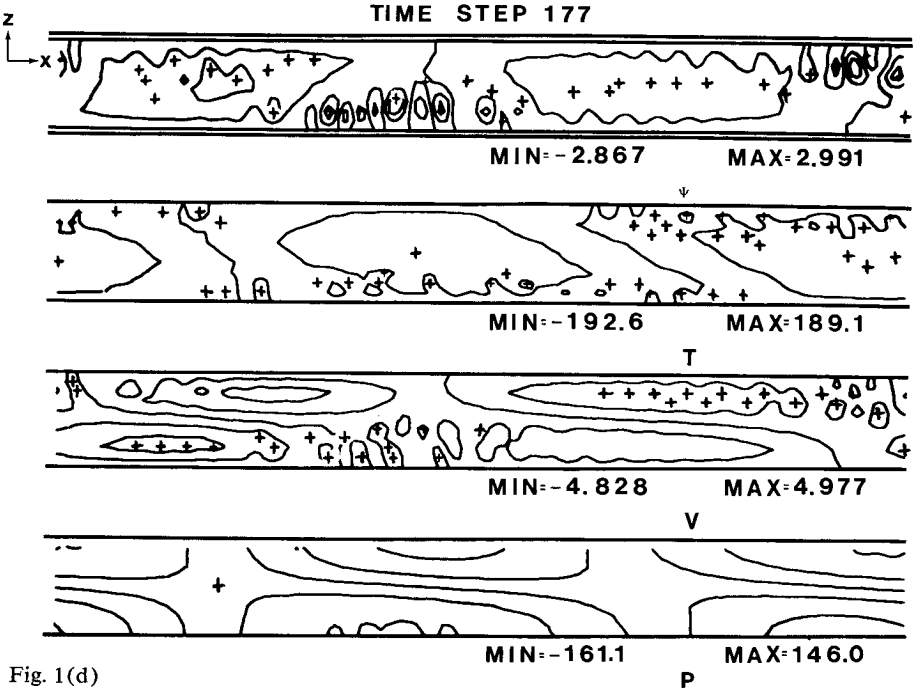

Fig. 1(d)

temperature (T); meridional velocity (v); and pressure (p). Local maxima are indicated by "+." Ranges (minimums and maximums) are given. Zero contours are labelled. The arrows indicate flow direction. The vertical distance is stretched in the boundary layers.

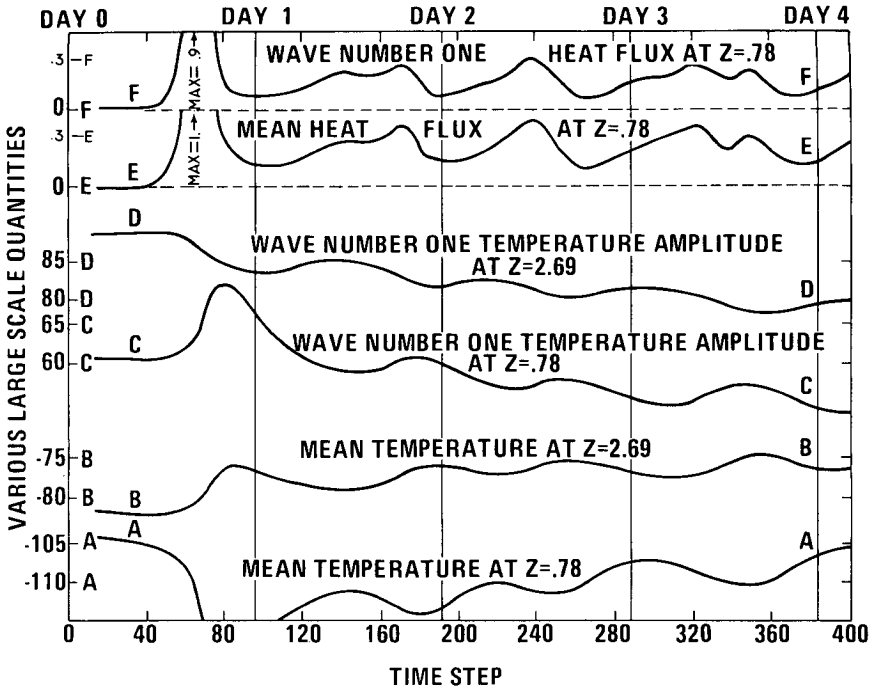

Fig. 2 Time dependence of six quantities. Abscissa is the stage three time step number. Ordinates corresponding to each of the six curves are indicated by letters A–F. The z-values given on each curve are model vertical coordinates using a vertical scale of ten units, with $z = 0$ at the bottom boundary. Curves E and F are total large-scale upward heat fluxes associated with the small-scale eddies; specifically,

$$\text{curve } E \propto \sum_{n=17}^{32} (W_n T_n^* + W_n^* T_n)$$

and

$$\text{curve } F \propto \left| \sum_{n=17}^{32} (W_n T_{n-1}^* + W_{n-1}^* T_n) \right|$$

where W_n and T_n are complex Fourier amplitudes of vertical velocity and temperature fields. Curves E and F are normalized relative to the maximum wave number 0 heat flux, which occurs at time step 68.

Arakawa and Schubert (1974) describe a nonlinear mechanism leading to what they call the "adjustment time scale," which could be associated with this time dependence. The mechanism involves the growth, nonlinear equilibration, and decay of convective ensembles in response to changes they induce in the large-scale static stability. Because of this nonlinearity, it may be difficult to explain the apparent natural period in the present results. In developing a nonlinear theory, one would have to consider changes in the large-scale "background" state, and the period would probably exhibit hysteresis effects depending on the initial state of the convective ensemble. Thus, it would be nice if a

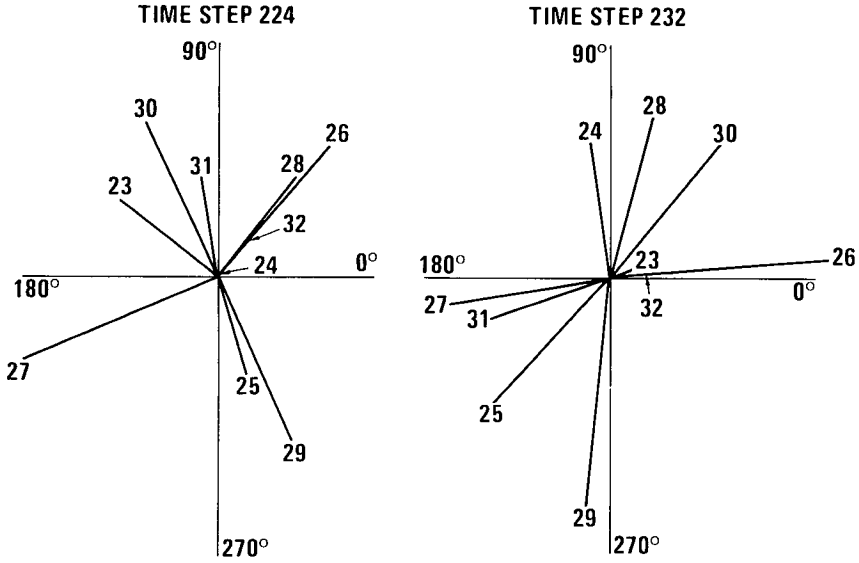

Fig. 3 Phase-plane diagrams showing amplitude and phase relations of most active small-scale eddy wave components (wave numbers 23–32) at time steps 224 and 232 of the stage-three time integration. Clockwise rotation of a vector from time step 224 to time step 232 corresponds to eastward phase propagation.

linear theory could explain the quasi-one-day oscillation in the present results and similar atmospheric phenomena.

The Arakawa-Schubert mechanism would be the likely explanation if there were significant one-day changes in the boundary-layer static instability (proportional to $\partial T/\partial z$). However, in the present results, both the mean and wave number one components of vertical temperature gradient vary by only about ± 5 per cent *even in the boundary layers*. There is no apparent mechanism by which such small variations could cause the much larger variations of convective ensemble flux in the boundary layers. (Evidence that the convective flux is not so sensitive to the large-scale flow was obtained from a run of the same case with all nonlinear interactions ignored except those involving or affecting the mean zonal flow. Although the static instability of the mean zonal flow is smaller by a factor of two than occurs under the cold dome of wave number one, the resulting mean zonal component of the convective ensemble heat flux is less by only a factor of two in this "reduced interaction" run.)

Thus, although there may be mechanisms for one-day oscillations of the large-scale flow (such as through nonlinear interactions with the convective ensemble or an inertia wave trapped in the statically unstable boundary layer), *the smallness of the time variations of the large-scale static stability in the present results suggests the explanation of the convective ensemble heat flux oscillation may not depend on such large-scale time variations.* A *possible* heuristic explanation not depending on such time dependence is as follows: the wave number one component heat transport is the net effect of contributions

from all wave number pairs of the form $(n, n + 1)$. Each pair corresponds to a given triad of interactions with a wave number one component. The phase velocities of the two small-scale components of each triad define a characteristic effective group velocity. This group velocity implies that small-scale energy in the interacting triad propagates relative to the long-wave environment. Since the large-scale static stability has a strong variation in its wave number one component, the small-scale energy is modulated by its interactions with the large scale as it propagates. The total wave number one heat transport, involving the net effect of all such triads, would also reflect such time dependence (but to a lesser degree, since the phase of the wave number one heat transport may vary from triad to triad). In the present problem, this time dependence is large at first, because the wave number one heat transport is nearly in phase for all pairs of small-scale wave numbers during the rapid initial growth of the small-scale convective band. Group velocity *variation* in the convective band gradually increases the variability of this phase, and the time dependence decreases.

This heuristic explanation assumes that most of the convective heat flux is associatiated with modes that have nearly the same (at least within a factor of two) group velocity. Otherwise, the time variation would be reduced to relatively small, nearly random fluctuations after the initial burst of activity. This raises the question of whether increasing the horizontal resolution would result in a wider wave number band of convective modes having significant heat transport and, if so, whether the group velocity would have large variation in the widened band. One way to reduce this possibility in the present simplified model is to use horizontal diffusion coefficients just large enough to significantly suppress wave numbers higher than the wave number most active in the absence of horizontal diffusion. Although the diffusion coefficients used in this study were chosen to be the right order of magnitude to significantly retard unresolved higher wave numbers, the high-resolution runs necessary to verify this choice have not yet been performed, because the high computation costs can be reduced by improved versions of the present model (as noted at the end of Section 3).

Whether this heuristic explanation offered for the present model time dependence may be relevant to atmospheric behaviour depends on whether there are significant cases (such as in east coast winter storms) where the convective modes transporting and releasing most of the latent heat have approximately uniform group velocity. If the active modes have a clear, characteristic horizontal scale, it is more likely that this will be true than if their energy is distributed over a wide range of scales.

The results shown in Fig. 3 indicate that the group velocities in the convective band are of the right order of magnitude to be consistent with this argument. That is, they are such that the energy propagates about one wave length (wave number one component) per model day. More convincing diagnostic evidence is difficult to obtain due to insufficient information on how the large scale modulates the small-scale convection in space *and* time. Separation of

dispersing gravity mode pairs having the same wave number[5] might make the phase plane vectors more regular, but this has not yet been attempted. Theoretical analysis is very difficult, because of the strong vertical and horizontal variations of static stability, which has both positive and negative values in the convective boundary layer, and also because there might be no valid linearization of the problem. The detailed structure and boundary-layer depth probably affect the group velocity significantly.

The key point is that there is significant time variation of the convective heat transport that is *apparently* not due to time variations of the large-scale flow. That is, the time variation would probably occur even if the large-scale flow were exactly steady. Apparently, *space variations of the large-scale environment can significantly modulate the convective heat transport in time as well as in space, whether or not the large-scale flow is steady.* Besides indicating the potential complexity of convective heat transport parameterization, especially after rapid growth of a convective ensemble, this leads to the interesting question of what might happen if the conditions were such that the frequency of large-scale convective heating were close to the corresponding large-scale inertia-gravity frequency. A rapid growth of convective ensemble heat transport and latent heat release will itself trigger a *large-scale* inertia-gravity oscillation due to accompanying large-scale pressure changes. In a rapidly growing east coast winter storm, simple scaling considerations (Brunet, 1974) suggest that such an oscillation might make a significant contribution to large-scale convergence and associated precipitation. (These scaling considerations indicate that the pressure changes associated with realistic convective heat transport and latent heat release in a growing convective ensemble can induce significant oscillating, out-of-balance, large-scale vertical motions.) Brunet (1974) studied large-scale rainfall data from Hurricane Agnes and found evidence for such an oscillation, although the effect on large-scale precipitation is rather small in that case.

Associated with this small-scale convective time dependence is relatively small time variation (about ±5 per cent) of large-scale fields, as shown by curves A, B, C, and D of Fig. 2. Convective ensemble heat transport and latent heat release may vary in a similar way in atmospheric disturbances with the ensemble changes being associated with relatively small changes of large-scale flow parameters. Note that such changes would be important in short-term convective precipitation probability forecasts.

As suggested by Fig. 3, the most active convection occurs in a band of wave numbers around wave number 27. However, wave number 32 grows the fastest *when interactions with only the mean zonal flow* are accounted for. This could be due to the unstable boundary-layer depth being less in the mean than it is under the "cold dome" of wave number one, thereby reducing the growth rates

[5]There are two primary gravity waves associated with each wave number, travelling in opposite directions.

of the lower wave numbers relative to wave number 32. This could also be due to wave number 32 (the highest represented wave number) having only one triad through which to obtain energy from wave number one, while the lower wave numbers have two. All waves have equal opportunity to interact with the mean flow.

The qualitative appearance of the fields shown in Fig. 1 suggests that there is relatively little activity in scales of motion between the large, quasi-geostrophic scale and the small, convective scale in the boundary layer. Fig. 4 confirms this quantitativity. Figs 4(a) and 4(b) are histograms revealing a strong gap in wave-number-band-averaged nonlinear heat transport interactions affecting large-scale temperature distribution. Fig. 4(c) shows a much less prominent gap in the temperature variance spectrum that, by itself, would suggest that the small-scale interactions are less important than indicated by Figs 4(a) and 4(b). However, the vertical velocity spectrum gives just the opposite picture, so that when one multiplies the RMS vertical velocity in each band by the corresponding RMS temperature, the resulting histogram is much more like Fig. 4(a) and Fig. 4(b) than is Fig. 4(c). Nevertheless, one should be very careful in making inferences from variance spectra alone, as these do not necessarily reflect the relative influence of different scales of motion on the large scales that are to be forecast. The reason is that phase relations, *averaged on the time scale of the large-scale eddies*, also influence the time-averaged vertical heat and momentum flux quantities.

The assumption of constant latitudinal temperature gradient used in the present model probably exaggerates the strength of the spectral gap indicated in Fig. 4, because this assumption eliminates the quasi-geostrophic cascade mechanism. Future studies should include this cascade mechanism, possibly within the framework of a two-dimensional model as mentioned in Section 2.

Finally, an interesting point about the structure of the convective eddies is that, while the vertical heat flux is predominantly upward, nonlinear inertia effects result in small downward flux on the interior side of unstable boundary layers. That is, fluid elements overshoot their equilibrium levels (where their temperature matches the large-scale environment temperature), so that upward moving fluid at the top of the lower boundary layer tends to be cooler than the average temperature at the same level. (This result has been observed by Deardorff et al., 1969, in laboratory experiments.) In fact, in the absence of dissipative effects and interaction with fluid at other levels, a fluid element would have its maximum vertical velocity at such an equilibrium level. Such downward heat transport cools the environment above the equilibrium level, thereby raising the equilibrium level for ensuing fluid elements. Thus, this nonlinear inertia effect deepens the convective boundary layer. It should also be noted that fluid deceleration above the equilibrium level generates gravity waves that can be important in momentum exchange with still higher levels. These nonlinear aspects of convective adjustment dynamics may be difficult to parameterize accurately in terms of large-scale flow parameters, although some schemes have been proposed for doing this (Deardorff et al., 1974). The

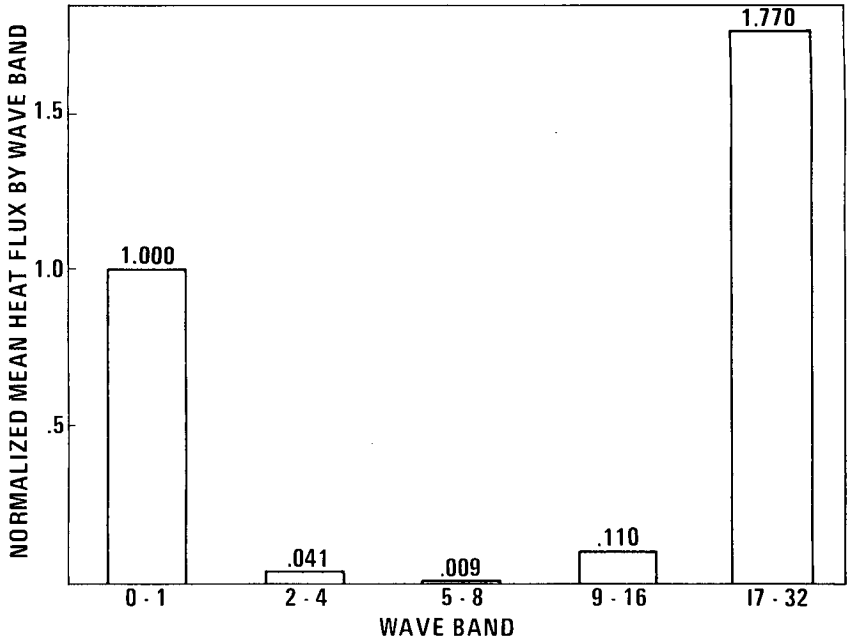

Fig. 4(a) Histogram showing time-averaged mean zonal heat transport by five individual bands of consecutive wave numbers. Horizontal scale of associated eddies decreases by about a factor of two for each bar proceeding left to right.

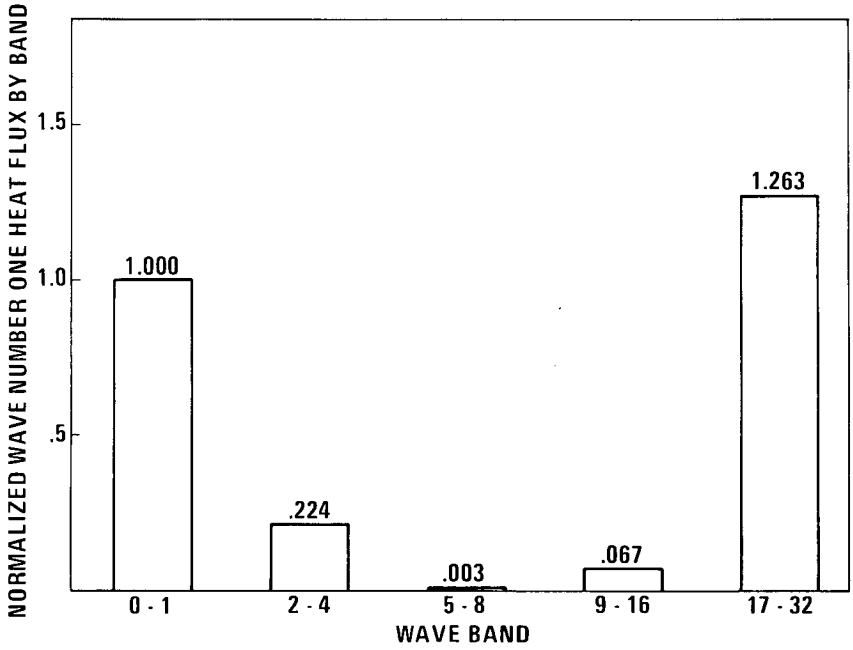

Fig. 4(b) Histogram showing amplitude of time-averaged wave number one heat transport by each of five bands of consecutive wave numbers.

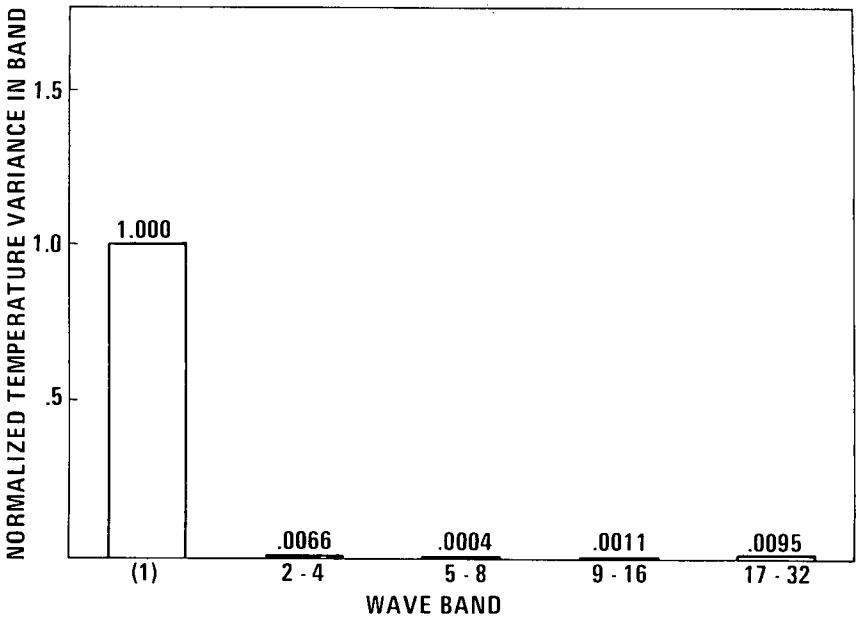

Fig. 4(c) Histogram showing temperature variance in each of five bands of consecutive wave numbers.

spectral gap approach advocated in Section I may prove superior to such classical parameterization approaches in representing such phenomena.

5 Concluding remarks

The results of this study suggest that using the full dynamic equations in spectral form to predict the interactions among large-scale atmospheric eddies and small-scale eddy ensembles, without having to represent intermediate-scale eddies, could be more realistic than using the usual parameterization approach. Specifically, the results of this simplified model of dry convective adjustment show:

(i) in this model, there is a clear spectral gap in the nonlinear interactions affecting large-scale eddies.

(ii) in this model, the nonlinear convective ensemble heat transport (i.e. the large-scale components of products of small-scale components of convective vertical velocity and small-scale components of temperature) apparently has significant *time* modulation, possibly due to ensemble energy propagation in a *space*-varying large-scale environment. The ensemble heat transport time variation appears independent of the time variations of the large-scale fields in the sense that the nonlinear transport apparently would vary significantly with time even if the large-scale fields were constant in time.

In view of (ii), the usual parameterization assumption that large-scale nonlinear transports are in a kind of quasi-equilibrium dictated by the large-scale fields (and possibly their recent histories) might not be accurate in general. In order to forecast these nonlinear transports, it may be necessary to specify initial values of both the large-scale fields and the large-scale nonlinear transport fields. If analogous convective ensemble time variation occurs in the atmosphere (as, for example, in east coast winter storms), the required large-scale initial distributions of nonlinear transport fields could, perhaps, be inferred from the intensity of small-scale oscillations (in space or time) recorded by observing stations.

Acknowledgments

During my recent service at McGill University, this research was supported by the National Research Council of Canada, under grant number 280-98, and by the Atmospheric Environment Service. More recently, it was supported by NAVAIR, under grant number NOO 173-76-C-0022. Computing support was provided by the National Center for Atmospheric Research. I am indebted to Drs Terry Williams, Steve Piacsek, Lothar Ruhnke, Jacques Derome, Harley Hurlburt, and Dana Thompson for valuable comments and assistance in the course of this research. I am especially indebted to Dr Tom Warn for valuable suggestions that gave the initial inspiration for this study. The fine technical assistance from Ms Karon Christensen and Ms Margaret Mikota in preparing this manuscript is greatly appreciated.

References

ARAKAWA, A. and W.H. SCHUBERT. 1974. Interaction of cumulus ensemble with the large-scale environment, Part I. *J. Atmos. Sci.* **31**: 674–701.

BATES, J.R. 1972. A generalization of CISK theory. *J. Atmos. Sci.* **30**: 1509–19.

BRUNET, N. 1974. Time spectral analysis of space-averaged precipitation. Master's thesis, McGill University, 78 pp.

CHARNEY, J.G. 1971. Geostrophic turbulence. *J. Atmos. Sci.* **28**: 1087–95.

——— and A. ELIASSEN. 1964. On the growth of the hurricane depression. *J. Atmos. Sci.* **21**: 68–75.

DEARDORFF, J.W.; G.E. WILLIS; and D.K. LILLY. 1969. Laboratory investigation of non-steady penetrative convection. *J. Fluid Mech.* **35**: 7–31.

———. 1974. Comments on the paper by A.K. Betts, "Non-precipitating cumulus convection and its parameterization." *Quart. J. Roy. Meteor. Soc.* **100**: 122–3.

DIETRICH, D.E. 1975. Numerical solution of fully implicit energy conserving primitive equations. *J. Meteor. Soc. Japan* **53**: 222–5.

———; B.E. MCDONALD; and A. WARN-VARNAS. 1975. Optimized block-implicit relaxation. *J. Comp. Phys.* **18**: 421–39.

HÖGSTRÖM, A.S. and U. HÖGSTRÖM. 1975. Spectral gap in surface-layer measurements. *J. Atmos. Sci.* **32**: 340–50.

LINDZEN, R.S. 1974. Wave-CISK in the tropics. *J. Atmos. Sci.* **31**: 156–79.

MCINTYRE, M.E. 1968. The axisymmetric convective regime for a rigidly bounded rotating annulus. *J. Fluid Mech.* **32**: 625–55.

NINOMIYA, K. 1975. Large-scale aspects of air-mass transformation over the East China Sea during AMTEX '74. *J. Meteor. Soc. Japan* **53**: 285–303.

OGURA, Y. 1964. Frictionally controlled, thermally driven circulations in a circular

vortex with application to tropical cyclones. *J. Atmos. Sci.* **21**: 610–21.

OOYAMA, K. 1964. A dynamic model for the study of tropical cyclone development. *Geofis. Intern.* (Mexico) **4**: 187–98.

WILLIAMS, G. 1969. Numerical integration of the three-dimensional Navier-Stokes equations for incompressible flow. *J. Fluid Mech.* **37**: 727–50.

WILLIAMS, R.T. 1967. Atmospheric frontogenesis: a numerical experiment. *J. Atmos. Sci.* **24**: 627–41.